IOPscience iopscience.iop.org

Home Search Collections Journals About Contact us My IOPscience

Triplet superconductivity in 3D Dirac semi-metal due to exchange interaction

This content has been downloaded from IOPscience. Please scroll down to see the full text.

2015 J. Phys.: Condens. Matter 27 025701

(http://iopscience.iop.org/0953-8984/27/2/025701)

View the table of contents for this issue, or go to the journal homepage for more

Download details:

IP Address: 140.113.38.11
This content was downloaded on 21/07/2015 at 09:33

Please note that terms and conditions apply.

IOP Publishing Journal of Physics: Condensed Matter
J. Phys.: Condens. Matter **27** (2015) 079501 (1pp) doi:10.1088/0953-8984/27/7/079501

Corrigendum: Triplet superconductivity in 3D Dirac semi-metal due to exchange interaction (2015 *J. Phys.: Condens. Matter* **27** 025701)

Baruch Rosenstein[1,2], B Ya Shapiro[3], Dingping Li[4,5] and I Shapiro[3]

[1] Department of Electrophysics, National Chiao Tung University, Hsinchu, Taiwan, People's Republic of China
[2] Applied Physics Department, Ariel University Center of Samaria, Ariel 40700, Israel
[3] Department of Physics, Institute of Superconductivity, Bar-Ilan University, Ramat-Gan 52900, Israel
[4] School of Physics, Peking University, Beijing 100871, People's Republic of China
[5] Collaborative Innovation Center of Quantum Matter, Beijing 100871, People's Republic of China

E-mail: vortexbar@yahoo.com

Received 12 January 2015
Accepted for publication 12 January 2015
Published 3 February 2015

We found missprints in two of our equations. In particular, equation (13) should be

$$\int_{\mathbf{r},\mathbf{r}'} \left[\psi^+_\alpha(r)\, M_{\alpha\beta}\psi^+_\beta(r)\,,\, \psi^+_\gamma\left(r'\right)\Sigma^i_{\gamma\delta}\psi_\delta\left(r'\right)\right]$$
$$= -\int_r \psi^+_\gamma(r)\left(\Sigma^i_{\gamma\delta}M_{\delta\kappa} + M_{\gamma\delta}\Sigma^{ti}_{\delta\gamma}\right)\psi^+_\kappa(r)\,.$$

while equation (15) should read

$$\Sigma_i T_j + T_j\Sigma^t_i = 2\mathrm{i}\varepsilon_{ijk}T_k.$$

 © 2015 IOP Publishing Ltd Printed in the UK

IOP Publishing Journal of Physics: Condensed Matter
J. Phys.: Condens. Matter **27** (2015) 025701 (13pp) doi:10.1088/0953-8984/27/2/025701

Triplet superconductivity in 3D Dirac semi-metal due to exchange interaction

Baruch Rosenstein[1,2], B Ya Shapiro[3], Dingping Li[4,5] and I Shapiro[3]

[1] Department of Electrophysics, National Chiao Tung University, Hsinchu, Taiwan, People's Republic of China
[2] Applied Physics Department, Ariel University Center of Samaria, Ariel 40700, Israel
[3] Department of Physics, Institute of Superconductivity, Bar-Ilan University, Ramat-Gan 52900, Israel
[4] School of Physics, Peking University, Beijing 100871, People's Republic of China
[5] Collaborative Innovation Center of Quantum Matter, Beijing 100871, People's Republic of China

E-mail: vortexbar@yahoo.com

Received 27 June 2014, revised 1 October 2014
Accepted for publication 18 November 2014
Published 15 December 2014

Abstract

Conventional phonon–electron interaction induces either triplet or one of two (degenerate) singlet pairing states in time reversal and inversion invariant 3D Dirac semi-metal. Investigation of the order parameters and energies of these states at zero temperature in a wide range of values of chemical potential μ, the effective electron–electron coupling constant λ and Debye energy T_D demonstrates that when the exchange interaction is neglected the singlet always prevails, however, in significant portions of the (μ, λ, T_D) parameter space the energy difference is very small. This means that interactions that are small, but discriminate between the spin singlet and the spin triplet, are important in order to determine the nature of the superconducting order there. The best candidate for such an interaction in the materials under consideration is the exchange (the Stoner term) characterized by constant λ_{ex}. We show that at values of λ_{ex}, much smaller than ones creating Stoner instability to ferromagnetism $\lambda_{ex} \sim 1$, the triplet pairing becomes energetically favored over the singlet ones. The 3D quantum critical point at $\mu = 0$ is considered in detail. This can be realized experimentally in optically trapped cold atom systems.

Keywords: Dirac semi-metals, unconventional superconductivity, exchange interaction

(Some figures may appear in colour only in the online journal)

1. Introduction

Recently, solids with electronic states described by the Bloch wave functions, obeying the 'pseudo-relativistic' Dirac equation (with Fermi velocity v_F replacing the velocity of light) attracted widespread attention. One outstanding example is graphene, a two-dimensional (2D) hexagonal lattice made of carbon atoms. The effective low-energy two-band model (near its K and K' points in the Brillouin zone) is described by the four-component (two pseudospins/sublattices and two valleys) massless 2D Dirac Hamiltonian (in fact there are two species of such quasiparticles for each spin). Although a similar two-band electronic structure of bismuth was described long ago by a four-component nearly massless Dirac fermion in 3D caused by spin–orbit interaction [1] (with spin replacing pseudospin), only recently several systems were experimentally found to exhibit the 3D Dirac quasiparticles. Their discovery followed recent exploration of the topological band theory [2].

One of the effective ideas to get a 3D Dirac semi-metal is to close the insulating gap by tuning a topological insulator towards the quantum phase transition to trivial insulators when the reflection symmetry is preserved [3]. The time reversal invariant 3D Dirac point in materials like Na_3Bi was theoretically investigated [4] and experimentally observed [5]. A well-known compound Cd_3As_2 is a symmetry-protected 3D Dirac semi-metal with a single pair of Dirac points in the bulk and nontrivial Fermi arcs on the surface [6, 7]. Most recently, conductivity and magneto-absorption of a zinc-blende crystal, HgCdTe, was measured [8] and is

 © 2015 IOP Publishing Ltd Printed in the UK

in agreement with theoretical expectations in Dirac semi-metal [9]. *Ab-initio* calculations and symmetry arguments predict [7] that crystallite BiO_2 exhibits Dirac points at three symmetry-related X points on the boundary of the FCC Brillouin zone. Perchlorate iridates [10] and inverse perovskites [11] were also predicted to be Weyl—semi-metals. Several known materials with well-known magnetic or transport properties have recently undergone a 'delayed' realization that they are actually Dirac semi-metals [12]. In addition, 3D Dirac semi-metal was realized in a cold atom system [13] (following the realization in 2D known as the 'synthetic graphene'). Interestingly, the sign and strength of the interaction can be controlled.

The discovery of the 3D Dirac materials makes it possible to study their physics including remarkable electronic properties. This is rich in new phenomena, not seen in 2D Dirac semi-metals like graphene and the surface states of a topological insulator harboring 2D Weyl quasiparticles. Examples include the giant diamagnetism that diverges logarithmically when the chemical potential approaches the 3D Dirac point; linear-in-frequency AC conductivity that has an imaginary part [9]; quantum magnetoresistance showing linear field-dependence in the bulk [11]. Most of the properties of these new materials were measured at relatively high temperatures. However, some of the topological insulators and suspected 3D Dirac semi-metals exhibit superconductivity at about the liquid He temperature.

The well-known topological insulator Bi_2Se_3 doped with Cu, becomes superconducting at $T_c = 3.8\,\mathrm{K}$ [14]. At present, its pairing symmetry is unknown. Some experimental evidence [15] points to a conventional phononic pairing mechanism. The spin-independent part of the effective electron-electron interaction due to phonons was studied theoretically [16, 17]. For a conventional parabolic dispersion relation, typically independent of spin, the phonon mechanism leads to the s-wave superconductivity. The layered, non-centrosymmetric heavy element $PbTaSe_2$ was found to be superconducting [18]. Its electronic properties like specific heat, electrical resistivity and magnetic-susceptibility indicate that $PbTaSe_2$ is a moderately coupled, type-II BCS superconductor with a large electron–phonon coupling constant of $\lambda = 0.74$. It was shown theoretically to possess a very asymmetric 3D Dirac point created by strong spin–orbit coupling. If the 3D is confirmed, it might indicate that the superconductivity is conventional phonon mediated.

More recently, when the Cu doped Bi_2Se_3 was subjected to pressure [19], T_c increased to 7 K at 30 GPa. Quasilinear temperature dependence of the upper critical field H_{c2}, exceeding the orbital and Pauli limits for the singlet pairing, points to the triplet superconductivity. The band structure of the superconducting compounds is apparently not very different from its parent compound Bi_2Se_3, so that one can keep the two band $\mathbf{k}\cdot\mathbf{p}$ description (Se p_z orbitals on the top and bottom layer of the unit cell mixed with its neighboring Bi p_z orbital). Electronic-structure calculations of the compound under pressure [19] reveal a single bulk three-dimensional Dirac cone like in Bi with large spin–orbit coupling. Usually the phonon mediated pairing leads to the s-wave 'conventional' superconductivity, while the p-wave pairing in $SrRuO_3$ or heavy fermion superconductors like UPt_3 'unconventional' non-phononic mechanism typically hinges on nonlocal interactions.

The case of the Dirac semi-metals is very special due to the strong spin dependence of the itinerant electrons' effective Hamiltonian. It was pointed out [20, 21] that in this case the triplet possibility can arise although the triplet gap is smaller than that of the singlet, the difference sometimes is not large for spin independent electron–electron interactions. Very recently, the spin-dependent part of the phonon induced electron–electron interaction was considered [22] and it was shown that the singlet is still favored over the triplet pairing. Another essential spin-dependent effective electron–electron interaction is the Stoner exchange among itinerant electrons [23] leading to ferromagnetism in transition metals. While in the best 3D Weyl semi-metal candidates it is too small to form a ferromagnetic state, it might be important to determine the nature of the superconducting condensate. Obviously, it favors the triplet pairing.

It is therefore important to clarify theoretically two questions. (i) Does a conventional phononic superconductivity exist in these materials with just a minute density of states compared even with high T_c cuprates that apparently utilize a much more powerful pairing mechanism than phonons offer? (ii) Is it possible that phonons in 3D Dirac materials lead to triplet pairing that even becomes dominant under certain circumstances?

In the present paper, we construct the theory of the superconducting transition in 3D Dirac semi-metal at arbitrary chemical potential including zero, assuming the local (probably, but not necessarily, phonon-mediated) pairing. The possible pairing channels are classified in this rather unusual situation using symmetries of the system. In contrast to the 2D case [24], the triplet pairing is not only possible, but for a moderately strong exchange interaction is the preferred channel taking over the more 'conventional' singlet one.

It turns out that the triplet superconductivity is more easily realized in the intriguing case of a small chemical potential. The superconductivity there is governed by a quantum critical point (QCP) [25]. The concept of QCP at zero temperature and varying doping constitutes a very useful language for describing the microscopic origin of superconductivity in high T_c cuprates and other 'unconventional' superconductors [26]. Quantum criticality, although occurring often in 2D (even in the context of surface superconductivity in topological insulators [27]), is very rare in 3D. We find and characterize the quantum critical points corresponding to both the singlet and the triplet superconducting transitions. There are experimental methods to tune the chemical potential by doping (for example by copper [14]), gating [28], pressure [19] etc. The Dirac semi-metal in optically trapped cold atom systems [13] is well suited to study this fascinating phenomenon.

The paper is organized as follows. The model of the phonon-mediated and exchange-effective local interactions of Dirac fermion is presented and the method of its solution (in the Gorkov equations form) including the symmetry analysis of possible pairing channels is given in section 2. In section 3 the

phase diagram for spin-independent interactions is established and the regions in parameter space where singlet and triplet states are nearly degenerate are identified. The Stoner exchange interaction is considered perturbatively in section 4. A novel case of zero chemical potential (QCP) is studied in section 5. Section 6 contains discussion on the experimental feasibility of the phonon-mediated superconductivity in 3D Dirac semi-metals, as well as a comparison with earlier calculations and conclusion.

2. The local pairing model in the Dirac semi-metal

2.1. Coulomb and electron–phonon interactions in the Dirac semi-metal

Electrons in the 3D Dirac semi-metal are described by field operators $\psi_{fs}(\mathbf{r})$, where $f = L, R$ are the valley index (pseudospin) for the left/right chirality bands with spin projections taking the values $s = \uparrow, \downarrow$ with respect to, for example, the z axis. To use the Dirac ('pseudo-relativistic') notations, these are combined into a four component bi-spinor creation operator, $\psi^\dagger = \left(\psi^\dagger_{L\uparrow}, \psi^\dagger_{L\downarrow}, \psi^\dagger_{R\uparrow}, \psi^\dagger_{R\downarrow}\right)$, whose index $\gamma = \{f, s\}$ takes four values. The non-interacting massless Hamiltonian with Fermi velocity v_F and chemical potential μ reads [4],

$$K = \int_{\mathbf{r}} \psi^+(\mathbf{r})\, \widehat{K}\psi(\mathbf{r}); \quad \widehat{K}_{\gamma\delta} = -i\hbar v_F \nabla^i \alpha^i_{\gamma\delta} - \mu\delta_{\gamma\delta}, \quad (1)$$

where three 4×4 matrices, $i = x, y, z$,

$$\boldsymbol{\alpha} = \begin{pmatrix} \boldsymbol{\sigma} & 0 \\ 0 & -\boldsymbol{\sigma} \end{pmatrix}, \quad (2)$$

are presented in the block form via Pauli matrices $\boldsymbol{\sigma}$. They are related to the Dirac γ matrices (in the chiral representation, sometimes termed 'spinor') by $\boldsymbol{\alpha} = \beta\gamma$ with

$$\beta = \begin{pmatrix} 0 & \mathbf{1} \\ \mathbf{1} & 0 \end{pmatrix}. \quad (3)$$

Here $\mathbf{1}$ is 2×2 identity matrix.

We consider a special case of 3D rotational symmetry that in particular has an isotropic Fermi velocity. Moreover we assume the time reversal, $\Theta\psi(\mathbf{r}) = i\sigma_y\psi^*(\mathbf{r})$ and inversion symmetries although the pseudo Lorentz symmetry will be explicitly broken by the interactions. The spectrum of single particle excitations is linear, see figure 1. The chemical potential μ is counted from the Dirac point.

Electrons interact electrostatically via the density–density potential $v(\mathbf{r})$:

$$V_{e-e} = \frac{1}{2}\int_{\mathbf{r}\mathbf{r}'} \rho(\mathbf{r})\, v(\mathbf{r}-\mathbf{r}')\, \rho(\mathbf{r}'); \quad \rho(\mathbf{r}) = \psi^+_\alpha(\mathbf{r})\,\psi_\alpha(\mathbf{r}) = \psi^+_{Ls}\psi_{Ls} + \psi^+_{Rs}\psi_{Rs}. \quad (4)$$

The interaction of the electrons with the ion's lattice vibrations is described by the phonon–electron coupling [29],

$$H_{e-ph} = w\int \rho(\mathbf{r})\, \boldsymbol{\nabla}\cdot\mathbf{u}(\mathbf{r}), \quad (5)$$

to overpower it to create the Cooper pairs as mentioned in the introduction. Here $\mathbf{u}(\mathbf{r})$ denotes the displacement of ions and the electron–ion coupling $w \propto M^{-1/2}$, where M is the ion mass.

2.2. Effective local Hamiltonian

The microscopic (Frőlich) Hamiltonian given by equations (1), (4) and (5) generally leads to long range effective electron–electron correlations and is to complicated to handle analytically. As usual, in certain cases the actual interaction can be approximated by a model local one. In these cases the effective electron–electron interaction due to both electron–phonon attraction and Coulomb repulsion (pseudopotential) can be expanded in derivatives. The leading term usually called the local (or the s-wave pairing) coupling is

$$V_{\text{eff}} = -\frac{g}{2}\int_{\mathbf{r}\mathbf{r}'} \rho(\mathbf{r})\,\delta(\mathbf{r}-\mathbf{r}')\,\rho(\mathbf{r}') = -\frac{g}{2}\int_{\mathbf{r}} \psi^+_\alpha(\mathbf{r})\,\psi^+_\beta(\mathbf{r})\,\psi_\beta(\mathbf{r})\,\psi_\alpha(\mathbf{r}). \quad (6)$$

Unlike the free Hamiltonian K, equation (1), this interaction Hamiltonian does not mix different spin components. Such a coupling implicitly restricts the spin-independent local interaction to be symmetric under the band permutation (the constants in front of the interband $\psi^\dagger_1\psi_1\psi^\dagger_2\psi_2$ and intraband $\psi^\dagger_1\psi_1\psi^\dagger_1\psi_1$ terms are the same). If the mechanism of pairing is due to acoustic phonons only, such an additional term is not generated. A more general case with an additional independent term was considered in [20]. Below we provide physical arguments that determine the validity range of this approximation.

The phonon part of the effective electron–electron coupling is local under very general circumstances since the scale on which the effective model is defined, $\hbar/\Lambda$, is typically larger than the range of phonon exchange $v_s/\omega_D \sim a$, where v_s is the velocity of sound and ω_D—Debye frequency and a—interatomic distance. The reason is that the physical condition on the cut-off scale of the theory is that it should be smaller than the size of Cooper pair ξ. The justification for using local interactions for initially long range Coulomb interaction is qualitatively different for two different cases: moderate electron density of the Dirac semi-metal and very small electron density.

(a) Generally for a moderately dense electron gas the electron repulsion does not prevent the phonon-mediated attraction if the characteristic electron–electron interaction time τ_e is smaller than the characteristic electron–phonon one, τ_{ph} (Coulomb suppression [29]). One can estimate the times for the Dirac electrons at chemical potential μ using the following arguments. For the Coulomb screening τ_e is related to the typical Coulomb energy e^2/r_s, where $r_s^{-3} \sim n$, n being the electron density, $\tau_e = \hbar r_s/e^2$. For the interaction with ionic lattice τ_{ph} is the inverse Debye frequency ω_D^{-1}, so that the crossover electron density when $\tau_e = \tau_{ph}$ is

$$n_{cr} = \frac{3}{4\pi}\left(\frac{T_D}{e^2}\right)^3, \quad (7)$$

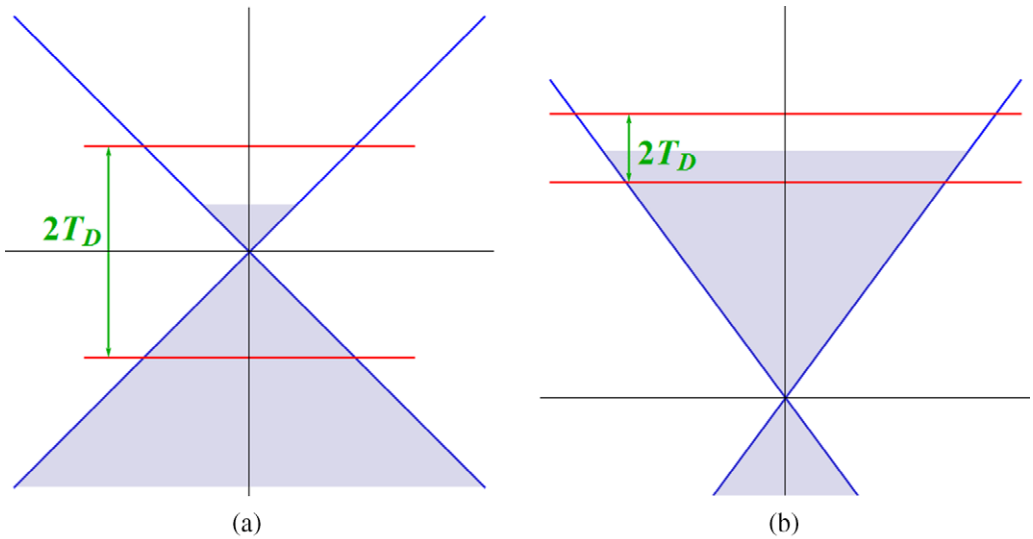

Figure 1. Chemical potential in Dirac semi-metals and the phonon-mediated pairing. (a) Chemical potential relative to Dirac point is smaller than typical energy of phonons, the Debye energy $T_{\rm D}$. (b) The BCS approximation limit: the chemical potential is much larger than the Debye energy $T_{\rm D}$.

where $T_{\rm D} = \hbar\omega_{\rm D}$. For $T_{\rm D} = 200\,{\rm K}$ (for [15] Bi_2Se_3) one requires $n_{\rm cr} = 4 \cdot 10^{14}\,{\rm cm}^{-3}$. For the linear dispersion relation of equation (1), this in turn leads to the minimal chemical potential for which the argument is valid:

$$\mu_{\rm cr} = \left(\frac{9\pi}{8}\right)^{1/3} v_{\rm F}\hbar\frac{T_{\rm D}}{e^2}. \tag{8}$$

Taking $v_{\rm F} \approx 7 \cdot 10^7\,{\rm cm\,s}^{-1}$ (for [22] Bi_2Se_3), one obtains $\mu_{\rm cr} = 100\,{\rm K} = 8\,{\rm meV} < T_{\rm D}$. Therefore, in this case the Coulomb pseudopotential just renormalizes the phonon contribution [29]. What happens when $\mu < \mu_{\rm cr}$? It is more involved.

(b) At small μ, namely for neutral, not charged plasma, the character of screening changes since the dominant mechanism becomes the polarization via the copious creation of the electron-hole pairs. In gapless Dirac semi-metals, despite the fact that the range of powerwise potential is large, its strength is greatly reduced. Even in the extreme case, $\mu = 0$, there is no static screening, although dynamically (within RPA [9]) large dielectric constant appears. Indeed in most materials that realize the Dirac semi-metals [8], there is a large dielectric constant $\varepsilon \sim 50$. This suppression of the direct Coulomb repulsion allows the Cooper pairing via the phonon-mediated attraction. Note that phonon screens the electric repulsion, but this effect is not dominant due to cancellation leading to the Migdal theorem, proved recently [30] for Dirac semi-metals. In the present paper, we restrict ourselves to the condition $\mu > \mu_{\rm cr}$ for a superconductor considering a special case $\mu = 0$ as an optically trapped cold atom model.

2.3. Exchange

Usually such an effective coupling with a positive coupling constant g leads to the s-wave 'conventional' pairing, while an 'unconventional' p-wave pairing in $SrRuO_3$ or heavy fermion superconductors like UPt_3 requires subleading interaction terms with two derivatives (most probably beyond electron–phonon mechanism). Two qualitatively different cases will be considered, see figure 1. When the chemical potential μ is much larger than the Debye energy $T_{\rm D}$ characterizing the outreach of the phonon–electron coupling, see figure 1(b), the physics is similar to that considered for the parabolic bands within the BCS approximations [29]. The opposite case, $\mu \ll T_{\rm D}$ (figure 1(a)) is unusual and most of our findings are devoted to this case.

The Coulomb forces in equation (4) in addition to direct repulsion lead to spin-dependent forces due to exchange. The exchange interaction among itinerant electrons first considered by Stoner [23], although small and unable to form a ferromagnetic state in materials under consideration, will be important for the nature of the condensate since it will lift the degeneracy between the singlet and the triplet pairing:

$$V_{\rm s-s} = -\frac{1}{2}\int_{\mathbf{r},\mathbf{r}'} J\left(\mathbf{r}-\mathbf{r}'\right)\mathbf{S}\left(\mathbf{r}\right)\cdot\mathbf{S}\left(\mathbf{r}'\right). \tag{9}$$

Spin density in Dirac semi-metal has the form

$$\mathbf{S}\left(\mathbf{r}\right) = \psi^{+}\left(\mathbf{r}\right)\boldsymbol{\Sigma}\psi\left(\mathbf{r}\right), \tag{10}$$

where the matrices

$$\boldsymbol{\Sigma} = -\boldsymbol{\alpha}\gamma_5 = \begin{pmatrix}\boldsymbol{\sigma} & 0\\ 0 & \boldsymbol{\sigma}\end{pmatrix}, \gamma_5 = \begin{pmatrix}-\mathbf{1} & 0\\ 0 & \mathbf{1}\end{pmatrix}, \tag{11}$$

are also the rotation generators.

2.4. The symmetry classification of possible pairing channels

Since we consider the local interactions as dominant, the superconducting condensate (the off-diagonal order parameter) will be local

$$O = \int_{\mathbf{r}} \psi^{+}_{\alpha}\left(\mathbf{r}\right) M_{\alpha\beta}\psi^{+}_{\beta}\left(\mathbf{r}\right), \tag{12}$$

where the constant matrix M should be a 4×4 antisymmetric matrix. Due to the rotation symmetry they transform covariantly under infinitesimal rotations generated by the spin S^i operator, equation (10):

$$\int_{\mathbf{r},\mathbf{r}'}\left[\psi^+_\alpha(r)\,M_{\alpha\beta}\psi^+_\beta(r)\,,\,\psi^+_\gamma\left(r'\right)\Sigma^i_{\gamma\delta}\psi_\delta\left(r'\right)\right]$$
$$=\int_r\psi^+_\gamma(r)\,\Sigma^i_{\gamma\delta}\left\{M^t_{\delta\kappa}-M_{\delta\kappa}\right\}\psi^+_\kappa(r)\,. \tag{13}$$

Here and in what follows 't' denotes the transpose matrix. The representations of the rotation group therefore characterize various possible superconducting phases.

Out of 16 matrices of the four dimensional Clifford algebra six are antisymmetric and one finds one vector and three scalar multiplets of the rotation group. The multiplets contain:

(a) a triplet of order parameters:

$$\left\{M^T_x,M^T_y,M^T_z\right\}=\{-\beta\alpha_z,-\mathrm{i}\beta\gamma_5,\beta\alpha_x\} \tag{14}$$

The algebra is

$$\left[M^T_i,\Sigma_j\right]=\mathrm{i}\varepsilon_{ijk}M^T_k\,. \tag{15}$$

(b) three singlets

$$M^S_1=\mathrm{i}\alpha_y;\quad M^S_2=\mathrm{i}\Sigma_y;\quad M^S_3=-\mathrm{i}\beta\alpha_y\gamma_5. \tag{16}$$

Which of the condensates is realized at zero temperature is determined by the parameters of the Hamiltonian and is addressed next within the Gaussian approximation.

3. The phase diagram for spin-independent interactions

3.1. Gor'kov equations

The BCS type approximation can be employed. Using the standard formalism, the Matsubara Green's functions (τ is the Matsubara time)

$$G_{\alpha\beta}\left(\mathbf{r},\tau;\mathbf{r}',\tau'\right)=-\left\langle T_\tau\psi_\alpha(\mathbf{r},\tau)\,\psi^\dagger_\beta\left(\mathbf{r}',\tau'\right)\right\rangle; \tag{17}$$
$$F^\dagger_{\alpha\beta}\left(\mathbf{r},\tau;\mathbf{r}',\tau'\right)=\left\langle T_\tau\psi^\dagger_\alpha(\mathbf{r},\tau)\,\psi^\dagger_\beta\left(\mathbf{r}',\tau'\right)\right\rangle,$$

obey the Gor'kov equations [29]:

$$-\frac{\partial G_{\gamma\kappa}\left(\mathbf{r},\tau;\mathbf{r}',\tau'\right)}{\partial\tau}-\int_{\mathbf{r}''}\left\langle\mathbf{r}\left|\widehat{K}_{\gamma\beta}\right|\mathbf{r}''\right\rangle G_{\beta\kappa}\left(\mathbf{r}'',\tau;\mathbf{r}',\tau'\right)$$
$$-gF_{\beta\gamma}(\mathbf{r},\tau;\mathbf{r},\tau)\,F^\dagger_{\beta\kappa}\left(\mathbf{r},\tau,\mathbf{r}',\tau'\right)$$
$$=\delta^{\gamma\kappa}\delta\left(\mathbf{r}-\mathbf{r}'\right)\delta\left(\tau-\tau'\right); \tag{18}$$
$$\frac{\partial F^\dagger_{\gamma\kappa}\left(\mathbf{r},\tau;\mathbf{r}',\tau'\right)}{\partial\tau}-\int_{\mathbf{r}''}\left\langle\mathbf{r}\left|\widehat{K}^t_{\gamma\beta}\right|\mathbf{r}''\right\rangle F^\dagger_{\beta\kappa}\left(\mathbf{r}'',\tau;\mathbf{r}',\tau'\right)$$
$$-gF^\dagger_{\gamma\beta}(\mathbf{r},\tau;\mathbf{r},\tau)\,G_{\beta\kappa}\left(\mathbf{r},\tau,\mathbf{r}',\tau'\right)=0.$$

In the homogeneous case the Gor'kov equations for Fourier components of the Greens functions simplify considerably [24],

$$D^{-1}_{\gamma\beta}G_{\beta\kappa}(\omega,p)-\Delta_{\gamma\beta}F^\dagger_{\beta\kappa}(\omega,p)=\delta^{\gamma\kappa}; \tag{19}$$
$$D^{-1}_{\beta\gamma}F^\dagger_{\beta\kappa}(\omega,p)+\Delta^*_{\gamma\beta}G_{\beta\kappa}(\omega,p)=0,$$

where $\omega=\pi T(2n+1)$ is the Matsubara frequency and $D^{-1}_{\gamma\beta}=(\mathrm{i}\omega-\mu)\,\delta_{\gamma\beta}+v_{\mathrm{F}}p^j\alpha^j_{\alpha\beta}$.

The matrix gap function can be chosen as

$$\Delta_{\beta\gamma}=gF_{\gamma\beta}(0)=gdM_{\gamma\beta}, \tag{20}$$

with real scalar d. These equations are conveniently presented in matrix form (superscript t denotes transposed and I—the identity matrix):

$$D^{-1}G-\Delta F^\dagger=I; \tag{21}$$
$$D^{t-1}F^\dagger+\Delta^*G=0.$$

Solving these equations one obtains

$$G^{-1}=D^{-1}+\Delta D^t\Delta^*; \tag{22}$$
$$F^\dagger=-D^t\Delta^*G,$$

with the gap function found from the consistency condition

$$\Delta^*=-g\sum_{\omega q}D^t\Delta^*G. \tag{23}$$

Now we find solutions of this equation for each of the possible superconducting phases.

3.2. Triplet solution of gap equation

In this phase rotational symmetry is spontaneously broken simultaneously with the electric charge $U(1)$ (global gauge invariance) symmetry. Assuming z direction of the p-wave condensate the order parameter matrix takes a form:

$$\Delta=\Delta_TM^T_z=\Delta_T\beta\alpha_x, \tag{24}$$

which is constant. In this section we use the units of $v_{\mathrm{F}}=1,\hbar=1$ and the energy scale will be set by the Debye cut-off, $T_{\mathrm{D}}=1$, of the electron–phonon interactions, see below. The off-diagonal (41) matrix element of the matrix gap equation, equation (23), for real $\Delta_T>0$ is:

$$\frac{1}{g}=\sum_{\omega q}\left[\Delta^2_T+p^2_\perp-p^2_z+\mu^2+\omega^2\right]$$
$$\times\left[\left(\Delta^2_T+\omega^2\right)^2+\left(p^2-\mu^2\right)^2+2\left(p^2+\mu^2\right)\omega^2\right.$$
$$\left.+2\Delta^2_T\left(p^2_\perp-p^2_z+\mu^2\right)\right]^{-1}, \tag{25}$$

where $p^2_\perp=p^2_x+p^2_y$. The spectrum of elementary excitations obtained from the four poles of the Green's function, see figure 2, is (in physical units)

$$E^2_\pm=\Delta^2_T+v^2_{\mathrm{F}}p^2+\mu^2\pm2v_{\mathrm{F}}\sqrt{\Delta^2_Tp^2_z+p^2\mu^2}. \tag{26}$$

There are two nodes at $p_x=p_y=0$, $v_{\mathrm{F}}p_z=\pm\sqrt{\Delta^2_T+\mu^2}$, when the branches $+|E_-|$ and $-|E_-|$ cross, see figure 2(*a*) and section $p_\perp=0$ in figure 2(*b*). There is also a saddle point with energy gap, $2\Delta_T$ on the circle $p^2_x+p^2_y=\mu^2$, $p_z=0$, see the section in the $p_z=0$ direction in figure 2(*c*). The higher

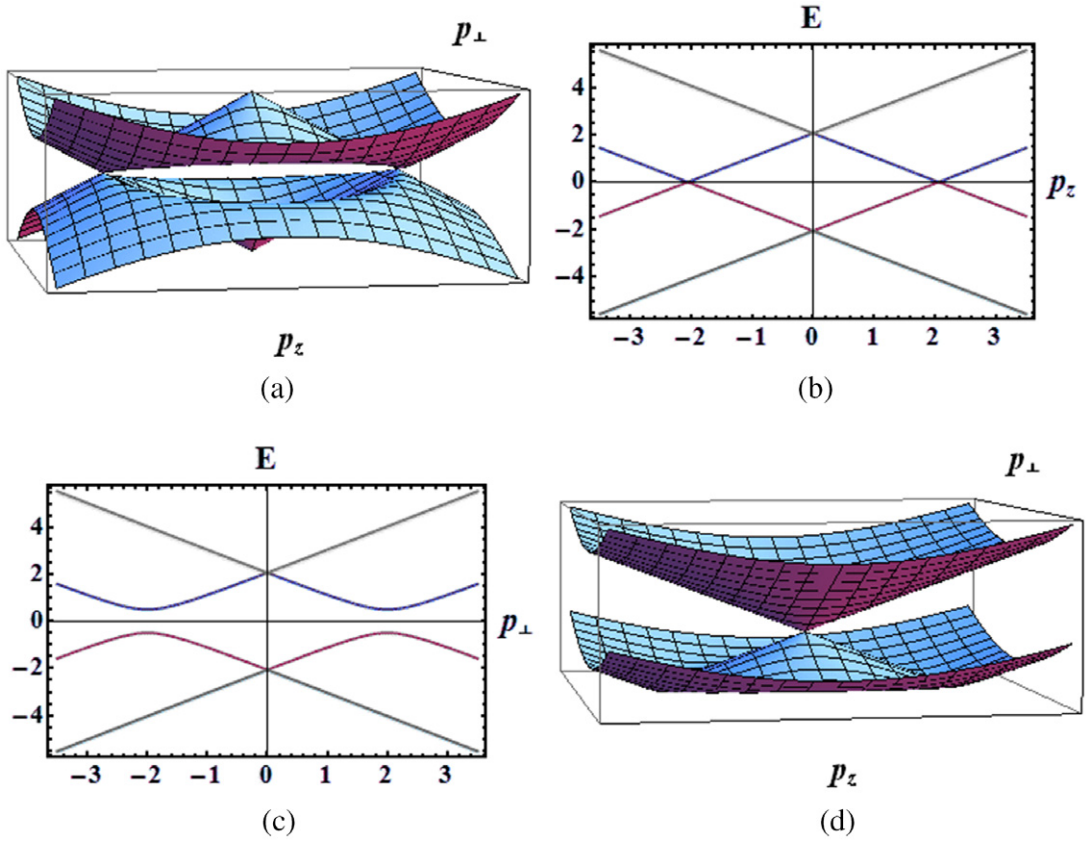

Figure 2. Spectrum of triplet excitations. (*a*) There are two nodes at $p_x = p_y = 0$, $v_F p_z = \pm\sqrt{\Delta_T^2 + \mu^2}$, when the branches $+|E_-|$ and $-|E_-|$ cross. (*b*) Section $p_\perp = 0$. (*c*) A saddle point with energy gap, $2\Delta_T$ on the circle $p_x^2 + p_y^2 = \mu^2$, $p_z = 0$. (*d*) The higher energy band E_+ touches the lower band at $p = 0$, so that there is a Dirac point for quasiparticles.

energy band E_+ touches the lower band at $p = 0$, so that there is a Dirac point for quasiparticles, see figure 2(*d*). Integration over ω, using polar coordinates for p and $x = \cos\theta$, $\zeta = \sqrt{\Delta_T^2 x^2 + \mu^2}$, gives

$$\frac{1}{g} = \frac{1}{8\pi^2}\int_{\max[\mu-1,0]}^{\mu+1} \mathrm{d}p \int_0^1 \mathrm{d}x \frac{p^2}{\zeta} \times \left\{ \frac{\zeta + px^2}{\sqrt{\Delta_T^2 + p^2 + \mu^2 + 2p\zeta}} + \frac{\zeta - px^2}{\sqrt{\Delta_T^2 + p^2 + \mu^2 - 2p\zeta}} \right\}. \tag{27}$$

The lower bound on the momentum integration is nonzero when the chemical potential μ exceeds T_D, see figure 2. The integral over x was performed analytically, while the last integral was done numerically. The result of the numerical solution of the gap equation for Δ_T is presented in figure 3(*a*). The lines of fixed g in the $\mu - \Delta_T$ plane are shown. As expected the gap increases as a function of μ. However, when the same is replotted as lines of fixed phonon–electron coupling,

$$\lambda = gD(\mu) = g\mu^2/\left(8\pi^2 v_F^3 \hbar^3\right), \tag{28}$$

the gap increases upon reduction in μ, see figure 3(*b*). At large $\mu \gg T_D$ the gap becomes independent of μ as in BCS, which is discussed next.

In several limiting cases the integrals can be performed analytically. At zero chemical potential the results are presented in section IV, while here we list the BCS limit of $\mu \gg T_D$ and the strong coupling case of $g\mu^2 \gg 1$, $\Delta_T \propto g$.

(i) In the BCS limit one has

$$\frac{1}{g} = \frac{a_T \mu^2}{4\pi^2} \sinh^{-1}\frac{T_D}{\Delta_T}, \tag{29}$$

with $a_T = 0.69$, leading to an exponential gap dependence on λ when it is small:

$$\Delta_T = T_D/\sinh(1/2a_T\lambda) \simeq 2T_D e^{-1/2a_T\lambda}. \tag{30}$$

(ii) In the strong coupling one obtains with solution

$$\Delta_T = \frac{g}{12\pi^2}\begin{cases} 6\mu^2 + 2 \text{ for } \mu < 1 \\ (\mu+1)^3 \text{ for } \mu > 1 \end{cases}, \tag{31}$$

see figure 3(*a*). Usually the local coupling does not prefer the triplet pairing and the singlet channels of coupling are realized. We therefore turn to them.

3.3. Singlet representations

It turns out that the second singlet in equation (16) gives results identical to that of the first one, while the third singlet does not have a solution in the physically interesting range of parameters. Therefore, we assume the order parameter in the matrix form $\Delta = \Delta_S M_1^S = i\Delta_S \alpha^y$. The relevant (41)

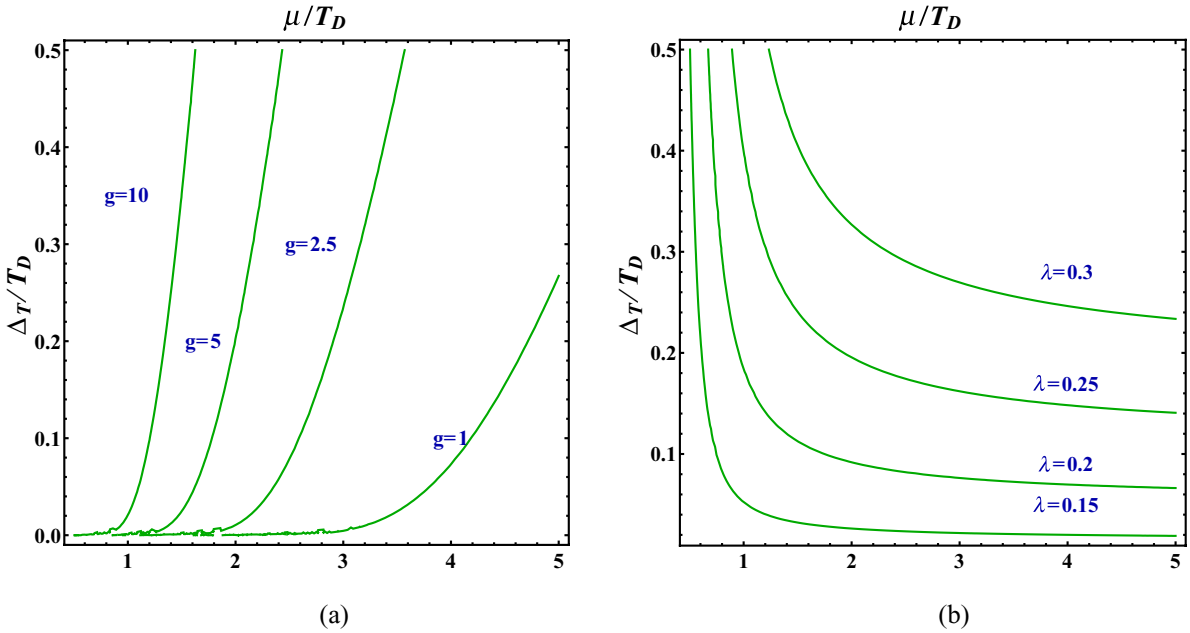

Figure 3. Triplet order parameter Δ_T. (a) as function of λ, (b) as function of g.

matrix element of the matrix gap equation, equation (23), is for real Δ_S:

$$\frac{1}{g} = \sum_{\omega p} \left[\Delta_S^2 + p^2 + \mu^2 + \omega^2\right] \times \left[\left(\Delta_S^2 + p^2\right)^2 + \left(\mu^2 + \omega^2 + 2\Delta_S^2\right)\left(\mu^2 + \omega^2\right) + 2p^2\left(\omega^2 - \mu^2\right)\right]^{-1}. \quad (32)$$

The spectrum (in physical units) now is isotropic,

$$E_\pm^2 = \Delta_S^2 + \left(v_F\,|p| \pm \mu\right)^2. \quad (33)$$

Integration over ω gives

$$\frac{1}{g} = \mu \sum_{\mu - T_D < \varepsilon_p < \mu + T_D} \frac{p}{r_+ r_- \left(r_+ - r_-\right)}, \quad (34)$$

where $r_\pm = \sqrt{\Delta_S^2 + (|p| \pm \mu)^2}$, while the p integration results in:

$$\frac{16\pi^2}{g} = \Phi\left(\mu + 1\right) - \Phi\left(\max\left[\mu - 1, 0\right]\right); \quad (35)$$

$$\Phi\left(p\right) = r_-\left(p + 3\mu\right) + r_+\left(p - 3\mu\right) - \left(\Delta_S^2 - 2\mu^2\right) \times \log\left[\left(p + r_- - \mu\right)\left(p + r_+ + \mu\right)\right].$$

The solution is presented in figures 4(a) and (b) as lines of constant g and λ, respectively. One observes that the gaps are comparable to those of the triplet shown in figure 3 in the whole range of parameters. The expression for the gap simplifies for

(i) BCS, $\mu \gg T_D$

$$\Delta_S = T_D / \sinh\left(1/2\lambda\right) \simeq 2T_D e^{-1/2\lambda}. \quad (36)$$

(ii) Strong coupling

$$\Delta_S = \frac{2\lambda\left(T_D + \mu\right)^3}{3\mu^2}. \quad (37)$$

Having found the order parameter, one has to determine what symmetry breaking is realized by comparing the energies of the solutions.

4. Singlet versus triplet

4.1. Energy

We calculate the energy of a solution using the well-known formula [29]

$$F = 2\int_{\Delta'=0}^{\Delta} \frac{\mathrm{d}\left(1/g\right)}{\mathrm{d}\Delta'}\Delta'^2. \quad (38)$$

For the triplet and singlet solutions the result of integration performed numerically is presented in figure 5(a). One observes that for all but the smallest coupling λ the channels are nearly degenerate although the singlet is always lower. The lines of constant difference $F_T - F_S$ are given in figure 5(b) as functions of μ and λ. The case of the quantum critical point $\mu = 0$ is analytically considered in detail in the following section.

In limiting cases, one obtains expressions in closed form.

(i) BCS, $\mu > T_D$, using equations (29) and (30) for the triplet and equation (36) for the singlet, one has the energy density:

$$F_{T,S} = -\frac{a_{T,S}\mu^2 T_D}{2\pi^2 v_F^3 \hbar^3}\left(\sqrt{\Delta_T^2 + T_D^2} - T_D\right) \simeq -\frac{a_{T,S}}{\pi^2}\frac{\mu^2 T_D^2}{v_F^3\hbar^3}\exp\left(-\frac{1}{a_{T,S}\lambda}\right), \quad (39)$$

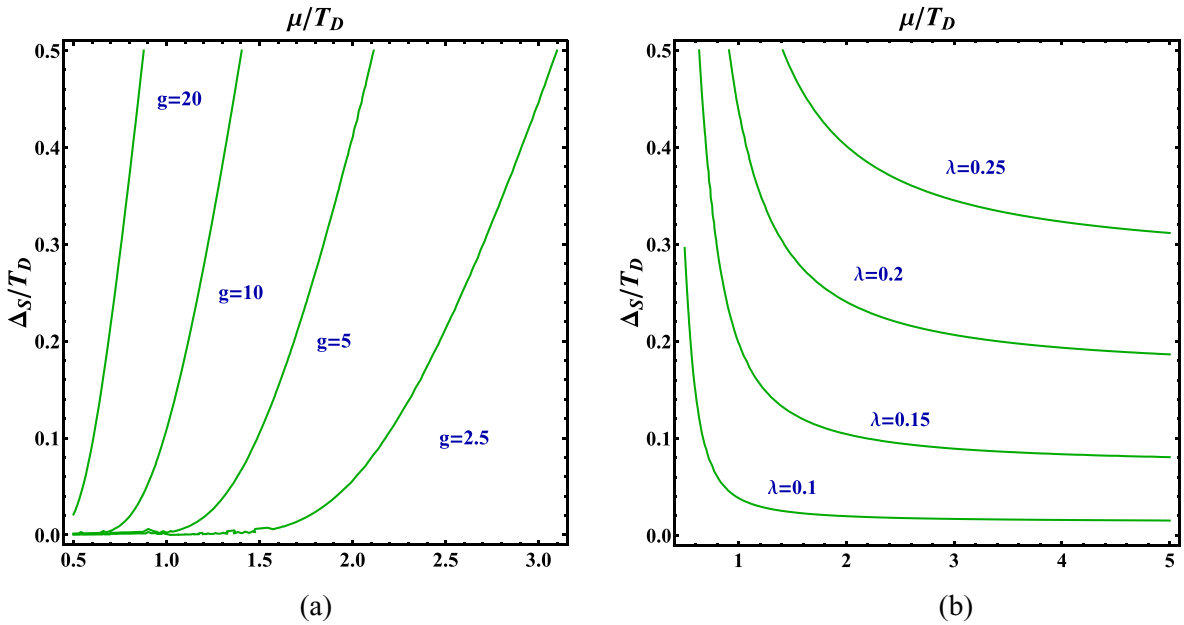

Figure 4. Singlet order parameter Δ_S. (a) as function of λ. (b) as function of g.

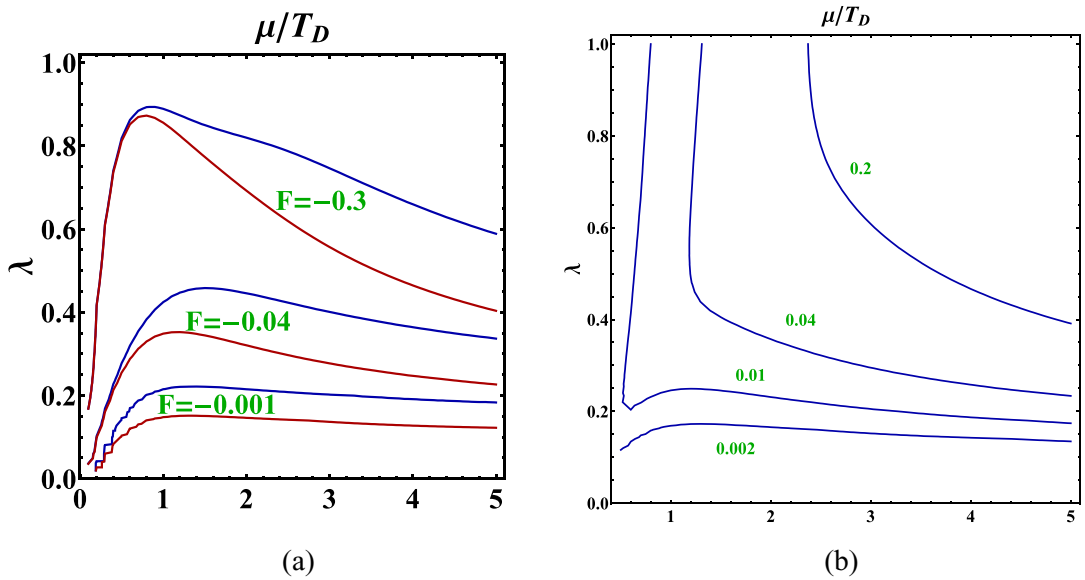

Figure 5. Energy of triplet and singlet. (a) Profile of constant energy for singlet and triplet condensates in the $\mu - \lambda$ plane. (b) Difference $F_T - F_S$.

with $a_T = 0.69$, while $a_S = 1$ and assuming $\lambda \ll 1$. The ratio of the two phases gives

$$\frac{F_T}{F_S} = 0.69 e^{-0.45/\lambda}. \tag{40}$$

(ii) Strong coupling limit, using equation (31) for triplet and equation (37) for the singlet,

$$F_T = F_S = -\frac{1}{72\pi^4 v_F^3 \hbar^3} \begin{cases} 4\left(3\mu^2 + T_D^2\right)^2 & \text{for } \mu < T_D \\ T_D^{-2}\left(\mu + T_D\right)^6 & \text{for } \mu > T_D. \end{cases} \tag{41}$$

The difference appears at order $1/g$.

To summarize, in most of the parameter range shown the triplet is a bit higher than that of the singlet, but the two condensates are nearly degenerate. The degeneracy in practice is lifted in favor of the triplet by the spin–spin interaction, equation (9), or magnetic impurities present in materials exhibiting the 3D Dirac point.

4.2. The influence of exchange

Let us estimate the perturbatively of the energy change due to the exchange interactions due to the Stoner exchange. In the simplest case of local spin attraction one uses the Stoner approximation [23], $J(\mathbf{r}) = I\delta(\mathbf{r})$, where I is the Stoner

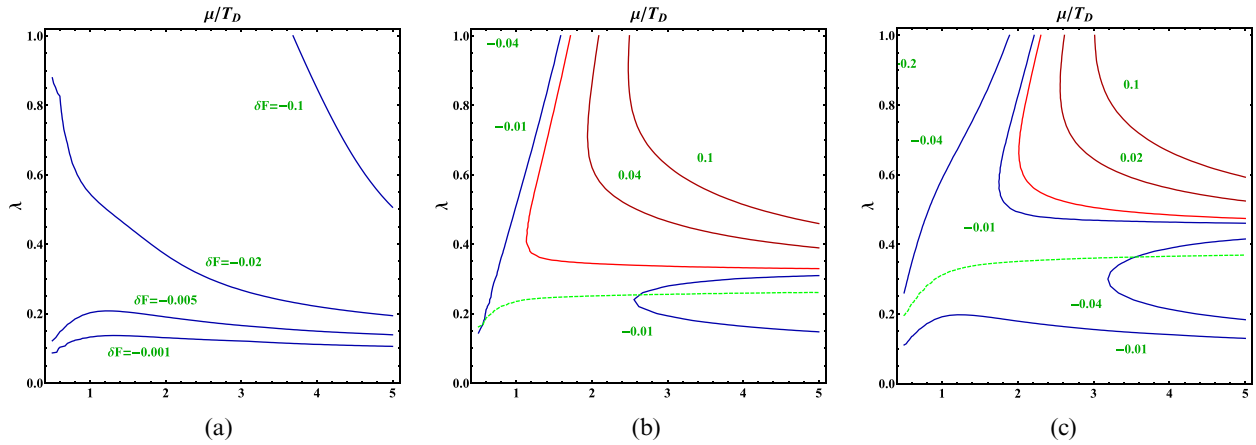

Figure 6. Comparison between energies of the singlet and triplet. (a) Exchange correction difference between the two channels: $\delta F = \delta F_T - \delta F_S$. ($b$) Difference of energies including the exchange correction for $\lambda_{ex} = 0.02$. The red line separates the singlet phase from the triplet phase. Above the line on the brown curves the energy difference $F_T - F_S$ is positive, while below it on the green line it is negative. Portion of the phase diagram below the dashed line requires consideration beyond perturbation theory. (c) Same for much larger exchange coupling $\lambda_{ex} = 0.32$.

constant, using the Gaussian factorization one obtains

$$\delta F = -\frac{I}{2V}\int_{\mathbf{r}} \Sigma^i_{\alpha\beta}\Sigma^i_{\gamma\delta}\left\langle \psi^+_\alpha(r)\,\psi_\beta(r)\,\psi^+_\gamma(r)\,\psi_\delta(r)\right\rangle \quad (42)$$
$$\simeq \frac{I}{2V}\int_{\mathbf{r}} \Sigma^i_{\alpha\beta}\Sigma^i_{\gamma\delta}\left\langle \psi^+_\alpha(r)\,\psi^+_\gamma(r)\right\rangle\left\langle \psi_\beta(r)\,\psi_\delta(r)\right\rangle$$
$$= \frac{I}{2g^2}\Delta^*_{\gamma\alpha}\Sigma^i_{\alpha\beta}\Delta_{\beta\delta}\Sigma^{it}_{\delta\gamma}.$$

The triplet, $\Delta = \Delta_T\beta\alpha^x$, predictably gains energy

$$\delta F_T = -\frac{2I}{g^2}\Delta_T^2, \quad (43)$$

while singlet, $\Delta = \mathrm{i}\Delta_S\alpha^y$ loses energy

$$\delta F_S = \frac{6I}{g^2}\Delta_S^2. \quad (44)$$

As in the case of the phonon-induced interactions, a more convenient dimensionless quantity describing the exchange is

$$\lambda_{ex} = ID(\mu) = I\mu^2/\left(8\pi^2 v_F^3\hbar^3\right). \quad (45)$$

We assume that the value is quite far from the Stoner ferromagnetic instability value ($\lambda_{ex} = 1$). The gain of the triplet over the singlet is therefore written as

$$\delta F_T - \delta F_S = -\frac{2\lambda_{ex}}{\lambda^2}D(\mu)\left(\Delta_T^2 + 3\Delta_S^2\right),$$

and is given in figure 6(a). The difference of full energies is given in figures 6(b) and (c) for two values of the exchange coupling. The crossover from singlet to triplet occurs, $F_T + \delta F_T = F_S + \delta F_S$ at the following value of the exchange coupling:

$$\lambda^c_{ex} = \frac{\lambda^2}{2D(\mu)}\frac{F_T - F_S}{3\Delta_S^2 + \Delta_T^2}. \quad (46)$$

Since perturbation theory in exchange coupling was used, the estimate is valid only when $F_{S,T} \gg \delta F_{S,T}$ marked by dashed lines on figures 6(b) and (c). On the lines the perturbation is half of the leading order. We argue that in this region either a ferromagnetic state is formed or the perturbation theory is not valid. In limiting cases analytic expression can be obtained.

(a) For $\mu \gg T_D$ according to equation (39)

$$F_T + \delta F_T = -8D(\mu)\,T_D^2\left(a_T + \frac{\lambda_{ex}}{\lambda^2}\right)e^{-1/a_T\lambda}; \quad (47)$$
$$F_S + \delta F_S = -8D(\mu)\,T_D^2\left(1 - 3\frac{\lambda_{ex}}{\lambda^2}\right)e^{-1/\lambda}.$$

Therefore, the transition occurs when

$$\lambda^c_{ex} = \lambda^2\frac{e^{(a_T^{-1}-1)/\lambda} - a_T}{3e^{(a_T^{-1}-1)/\lambda} + 1} \approx \frac{\lambda^2}{3}. \quad (48)$$

(b) In the strong coupling for $\mu < T_D$, $\Delta_T = \Delta_S \sim \frac{T_D^4}{18\pi^4 v_F^3\hbar^3}$, so that the difference is

$$\delta F_T - \delta F_S \sim -\frac{32}{9\pi^2}\frac{\lambda_{ex}T_D^4}{\mu^2}. \quad (49)$$

The triplet is always favored in this limit due to degeneracy of energies without the exchange coupling.

Critical exchange coupling for various chemical potential and the phonon-induced electron–electron coupling is presented in figure 7. As was mentioned in the introduction, the 'extreme' case of zero chemical potential can be physically achieved by tuning parameters of the material to the transition between the topological insulator phase and the band insulator phase, so that we can study it in more detail.

5. Quantum critical point at zero chemical potential and Its critical exponents

A peculiarity of superconductivity in Dirac semi-metal at zero chemical potential is that electrons (and holes) in Cooper pairs are created themselves by the pairing interaction rather than being present in the sample as free electrons. Therefore, it is

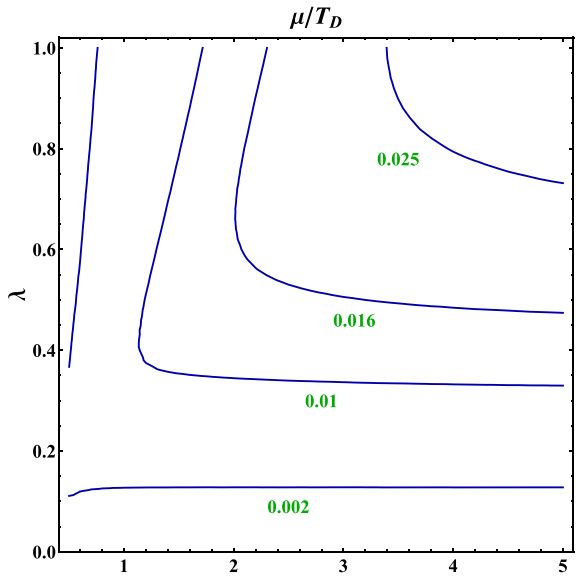

Figure 7. Critical exchange coupling for various chemical potential μ and the phonon-induced electron–electron coupling λ.

shown that it is possible to neglect the effect of weak doping and consider directly the $\mu = 0$ particle-hole symmetric case. This point in parameter space is the QCP [25]. Microscopically, Cooper pairs of both electrons and holes are formed. The system is unique in this sense since the electron-hole symmetry is not spontaneously broken in both normal and superconducting phases. Supercurrent in such a system does not carry momentum or mass. We discuss the triplet state followed by the singlet.

5.1. Triplet

The spectrum of the triplet becomes very simple, $E_{\pm}^2 = (\Delta_T \pm v_F |p_z|)^2 + v_F^2 p_\perp^2$. Performing analytically the integral over the angle and the momentum in the gap equation, equation (27), one obtains

$$\frac{12\pi^2 v_F^3 \hbar^3}{g} = \begin{cases} T_D^2 - \frac{\Delta_T^2}{5} & \text{for } \Delta_T < T_D \\ \frac{T_D^3}{\Delta_T} - \frac{T_D^5}{5\Delta_T^3} & \text{for } \Delta_T > T_D \end{cases} . \quad (50)$$

The solution of the equation for Δ_T as a function of coupling g is presented in figure 8(a). The triplet superconducting solution exists, as in the 2D case [27], only when the coupling exceeds a critical value (in physical units),

$$g_c^T = 12\pi^2 \frac{v_F^3 \hbar^3}{T_D^2}. \quad (51)$$

The dependence on the cut-off T_D is incorporated in the renormalized coupling with the dimension of energy defined as

$$U_T^2 = T_D^2 \left(1 - \frac{g_c^T}{g}\right). \quad (52)$$

This quantity can be interpreted as an effective binding energy of the Cooper pair in the Dirac semi-metal. The dependence of the gap is $\Delta_T = \sqrt{5} U_T$ for $U_T < 5^{-1/2}$ (or $g < 5/4 g_c^T$). The critical exponent therefore is $\Delta_T \propto \left(1 - g_c^T/g\right)^\beta$ for $\beta = 1/2$. This defines the (zero temperature) triplet quantum critical point.

Energy, calculated using the AGD formula, equation (38), can be written via the energy gap in a closed form:

$$F_T = -\frac{T_D^2}{5 g_c^T} \begin{cases} \frac{\Delta_T^4}{T_D^4} & \text{for } \Delta_T < T_D \\ 10\frac{\Delta_T}{T_D} - 15 + \frac{6T_D}{\Delta_T} & \text{for } \Delta_T > T_D \end{cases} . \quad (53)$$

Near criticality, equation (53), $F_T \propto \left(1 - g_c^T/g\right)^{2-\alpha}$, determines the quantum critical exponent $\alpha = 2$. Critical exponents coincide with the classical mean field 3D exponents.

In the strong coupling limit $\Delta_T = T_D g/g_c^T$ and $F_T = -2g T_D^2/\left(g_c^T\right)^2$. As can be seen in the next subsection, the triplet QCP is unstable since the singlet order parameter solution has lower energy.

5.2. Singlet

The spectrum is relativistic with the rest mass equal to the gap, $E^2 = \Delta_S^2 + v_F^2 p^2$. The gap equation after integrations is

$$\frac{8\pi^2 v_F^3 \hbar^3}{g} = T_D \sqrt{\Delta_S^2 + T_D^2} - \Delta_S^2 \sinh^{-1}(T_D/\Delta_S). \quad (54)$$

The critical value is therefore lower than that for the triplet

$$g_c^S = 8\pi^2 \frac{v_F^3 \hbar^3}{T_D^2}. \quad (55)$$

In terms of the renormalized coupling, $U_S^2 = T_D^2 \left(1 - \frac{g_c^S}{g}\right)$, the gap equation near criticality takes the form

$$U_S^2 = \Delta_S^2 \log\left(\frac{2T_D}{\sqrt{e}\Delta_S}\right). \quad (56)$$

The solution of equation (54) is given in figure 8(a) (red curve).

At small deviations from criticality one can approximate the solution as $\Delta_S = U_S \log^{-1/2}\left(2T_D/\sqrt{e}U_S\right)$, while in the strong coupling limit, $\Delta_S = \frac{2g}{3g_c^S} T_D$. The energy is

$$F_S = \frac{2T_D}{g_c^S}\left(T_D - \sqrt{\Delta_S^2 + T_D^2}\right) + \frac{1}{g}\Delta_S^2. \quad (57)$$

Near critical coupling, $F_S \simeq -\frac{U_S^4}{T_D^2 g_c^S} \log^{-1}\left(2T_D/\sqrt{e}U_S\right)$, while in the strong coupling limit one obtains again degeneracy with the triplet, $F_S = F_T = -8T_D^2 g/\left(3g_c^S\right)^2$, see figure 8 where blue and red curves correspond to triplet and singlet states.

5.3. The singlet triplet crossover due to exchange interaction

When the exchange interaction is added perturbatively (at coupling above the critical one for the triplet), the energies of the competing condensates are shifted; the crossover exchange (Stoner) coupling constant I, defined in equation (20), is given in figure 9 as the function of the electron–electron local coupling g. For g just above the critical for triplet g_c^T, see equation (51), the value of the I_c is about $I_c = 6$ (in units

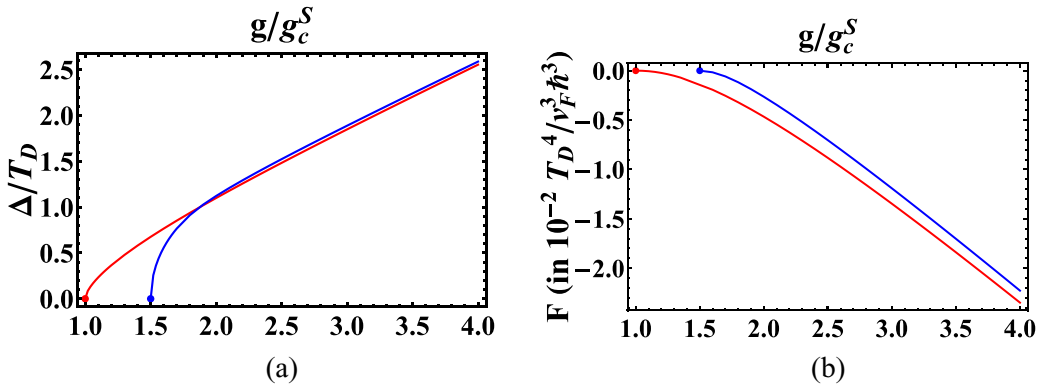

Figure 8. Quantum critical point $\mu = 0$. (a) Singlet and triplet order parameter as function of g. (b) Energies.

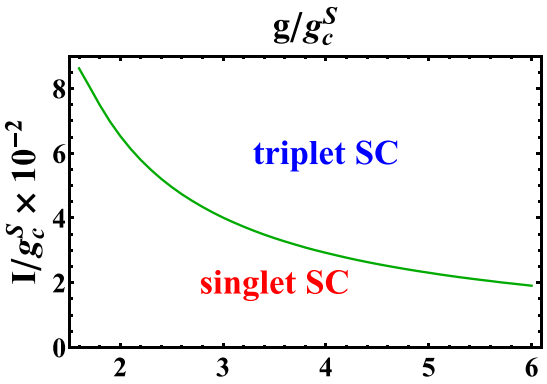

Figure 9. Critical exchange coupling as function of g at quantum critical point.

of $v_F^3\hbar^3/T_D^2$), so that $I_c = \frac{6}{12\pi^2} = 0.05$. As the phonon-mediated attraction strength increases the critical value of exchange decreases as $1/g$.

The Dirac superconductor therefore is a rare example of 3D quantum critical point.

6. Discussion and conclusions

6.1. Summary

To summarize, we have constructed a microscopic theory of superconductivity (at zero temperature) in 3D time reversal and inversion invariant massless Dirac semi-metals. In these materials there are at least two bands of opposite chiralities. Such a band structure appears in many recently studied materials including copper doped TI Bi_2Se_3 in which the triplet superconductivity is suspected [19].

In the framework of the 'conventional' phonon-mediated local attraction model we classified, under simplifying assumptions of the 3D rotation invariance, inversion and the time reversal, possible pairing channels. There are three singlet channels and one triplet. The comparison of energies of these condensates for arbitrary chemical potential and the electron–electron interaction strength demonstrates that a singlet pairing always prevails, as shown in figure 5. However, one notices that in large portions of the phase diagram the energy density differences are much smaller that the typical values of energy densities themselves. This means that interactions that are small but discriminate between the spin singlet and the spin triplet are important in order to determine the nature of the superconducting order there.

The best candidate for such an interaction in materials under consideration is the exchange (the Stoner term). Parameters of the model are therefore the chemical potential μ, the effective electron–electron coupling strength g and the Stoner coupling exchange constant I. Our main results are given in figure 6. In certain ranges of parameters that include the electron–phonon coupling parametrized by dimensionally effective electron–electron coupling λ and the exchange interaction parametrized by λ_{ex}, the triplet pairing is favored over the singlet one. Figures 6(b) and (c) demonstrate that the triplet exists either at small chemical potential of order Debye energy T_D or perhaps as small λ and large chemical potential, while the singlet prevails in the upper-right corner of the diagram beyond the red line.

The second region where the triplet is competitive happens to be beyond the range of validity of the perturbation theory and in fact will not materialize since the superconducting order instability is probably weaker than the Stoner instability for ferromagnetic correlations, so we are left with the triplet states when the chemical potential is small.

To this end we have investigated the limit of zero chemical potential, where the tendency towards the triplet pairing should be maximal. This is presented in figure 9. In this limit one cannot use the dimensionless coupling strengths λ and λ_{ex}, therefore should go back to the dimensional coupling strengths g and I related to the former by equations (28) and (45) used in this phase diagram. Transition to superconductivity in this case is a rare occurrence of quantum critical point in 3D with distinct critical couplings and exponents.

6.2. Experimental feasibility of the triplet superconductivity due to phonon and exchange interactions

To estimate the pairing efficiency due to phonons, one should rely on recent studies [22]. The effective dimensionless electron–electron coupling constant due to phonons λ, defined in equation (28), is obtained from the exchange of acoustic phonons and is of the order of [18] 0.1–1 (somewhat lower values are obtained in [17]). Note that a reasonable electron

density of $n = 3 \cdot 10^{11}$ cm^{-2} in Bi_2Te_3 already conforms to the requirement that chemical potential less than the Debye cut-off energy $T_D = 200$ K.

To estimate the strength of the exchange interactions due to itinerant electrons one, as usual, we start from the Coulomb repulsion. The effects of Coulomb interaction in 3D Dirac electrons are being studied extensively [9]. RG analysis reveals the logarithmic divergence of Fermi velocity v_F, while the effective fine structure constant $\alpha = e^2/\hbar v_F$ is marginally irrelevant. When a Dirac point is located on the Fermi level, the Coulomb interaction is not screened. The Stoner theory [23] predicts that when λ_{ex} becomes of the order of 1, the material develops ferromagnetism. Below that only the correlations play a role, but as is seen in figures 6(*a*) and (*b*), such a relatively small exchange is sufficient to damage the singlet condensate in favor of the triplet.

6.3. Feasibility of observing the quantum criticality

In this paper we especially focused on the qualitatively distinct case of Dirac fermions with small chemical potential. The situation is quite similar to that of the 2D Weyl semi-metal in topological insulators. Although in the original proposal of TI in materials [31] the chemical potential was zero, in experiments one finds often that the Dirac point is shifted away from the Fermi surface by a significant fraction of eV [2]. There are however experimental methods to shift the location of the point by doping (for example by copper [14]), gating, pressure, etc. [28]. Superconductivity was in fact observed in otherwise non-superconducting TIs Bi_2Te_3 and Bi_2Se_3 under pressure [19]. It is possible that at a certain pressure the system passes through the quantum critical point and is therefore a candidate for the maximal enhancement of the triplet superconductivity. The Dirac semi-metal in optically trapped cold atoms [13] offers a well-controllable system in which this phenomenon occurs both for repulsive interaction (chiral symmetry breaking) and the attractive one (superconductivity). The measurable quantity would be the p-wave or the s-wave condensate.

6.4. Possible generalizations and comparison with other works

Here we compare our results with the earlier work [20] designed to model the symmetries and parameters of Cu doped Bi_2Se_3. The case that can be directly compared is when the relativistic mass term (denoted by m in [20]) is small compared to chemical potential. In this work a more general effective electron–electron interaction was considered with two couplings V and U for local intraband and interband attractions, respectively. They are related to our g by $g = 2U = 2V$. Qualitatively, for $U/V = 1$ one gets nearly degenerate energies (critical temperatures were compared in [20] instead). This is similar but not identical to our result without exchange, see figure 6. We indeed obtain the degeneracy of the two gaps, the singlet and the triplet (their Δ_1 and Δ_2 respectively), but only in the limit of large g. The gaps are definitely not degenerate when the coupling g is below $20\pi^2 v_F^3 \hbar^2 / T_D^2$. Even within the BCS regime (equations (36) and (30)), $\Delta_T/\Delta_S = \sinh(0.35/\lambda)/\sinh(0.5/\lambda)$. This is consistent with 1 only for quite large coupling (whatever UV cut-off is used in [20]).

The physics of the triplet superconductors of this type is very rich and has already been investigated in connection with heavy fermion superconductors. In particular, their magnetic vortices appear as either vector vortices or so-called skyrmions [32]—coreless topologically nontrivial textures. In particular, their magnetic properties like the magnetization are very peculiar and even without magnetic field the system forms a 'spontaneous flux state'. The material therefore can be called a 'ferromagnetic superconductor'. The superconducting state develops weak ferromagnetism and a system of alternating magnetic domains [32].

Acknowledgments

We are indebted to C W Luo, J J Lin and W B Jian for explaining details of experiments and T Maniv and M Lewkowicz for valuable discussions. The work of Baruch Rosenstein and Dingping Li was supported by the NSC of ROC Grant No. 98-2112-M-009-014-MY3 and the MOE ATU program. The work of Dingping Lee was also supported by the National Natural Science Foundation of China (No. 11274018)

References

[1] Wolff P A J 1964 *Phys. Chem. Solids* **25** 1057
[2] Hasan Z and Kane C L 2010 *Rev. Mod. Phys.* **82** 3045
Qi X-L and Zhang S-C 2011 *Rev. Mod. Phys.* **83** 1057
Bernevig B A 2013 *Topological Insulators and Topological Superconductors* (Princeton: Princeton University Press)
[3] Young S M, Chowdhury S, Walter E J, Mele E J, Kane C L and Rappe A M 2011 *Phys. Rev.* B **84** 085106
[4] Wang Z, Sun Y, Chen X-Q, Franchini C, Xu G, Weng H, Dai X and Fang Z 2012 *Phys. Rev.* B **85** 195320
Hosur P, Dai X, Fang Z and Qi X-L 2014 *Phys. Rev.* B **90** 045130
[5] Liu Z K *et al* 2014 *Science* **343** 864
Xu S-Y *et al* 2013 Observation of a bulk 3D Dirac multiplet, Lifshitz transition and nestled spin states in Na_3Bi arXiv:1312.7624
[6] Xu G, Weng H, Wang Z, Dai X and Fang Z 2011 *Phys. Rev. Lett.* **107** 186806
Wang Z, Weng H, Wu Q, Dai X and Fang Z 2013 *Phys. Rev.* B **88** 125427
Neupane M *et al* 2014 *Nat. Commun.* **5** 3786
[7] Young S M, Zaheer S, Teo J C Y, Kane C L, Mele E J and Rappe A M 2012 *Phys. Rev. Lett.* **108** 140405
[8] Orlita M *et al* 2014 *Nat. Phys.* **10** 233
[9] Fuseya Y, Ogata M and Fukuyama H 2009 *Phys. Rev. Lett.* **102** 066601
Hosur P, Parameswaran S A and Vishwanath A 2012 *Phys. Rev. Lett.* **108** 046602
Lewkowicz M and Rosenstein B 2013 *Phys. Rev.* B **88** 045108
Rosenstein B, Kao H C and Lewkowicz M 2014 *Phys. Rev.* B **90** 045137
Lv M and Zhang S-C 2013 *Int. J. Mod. Phys.* B **27** 1350177
[10] Hosur P, Ryu S and Vishwanath A 2010 *Phys. Rev.* B **81** 045120
Wan X, Turner A M, Vishwanath A and Savrasov S Y 2011 *Phys. Rev.* B **83** 205101

Witczak-Krempa W and Kim Y B 2012 *Phys. Rev.* B **85** 045124
[11] Kariyado T and Ogata M 2011 *J. Phys. Soc. Japan* **80** 074704
Kariyado T and Ogata M 2012 *J. Phys. Soc. Japan* **81** 064701
Delplacel P, Li J and Carpentier D 2012 *Europhys. Lett.* **97** 67004
[12] Timusk T, Carbotte J P, Homes C C, Basov D N and Sharapov S G 2013 *Phys. Rev.* B **87** 235121
[13] Dan-wei Z, Zi-dan W and Shi-liang Z 2012 *Front. Phys.* **7** 31
[14] Hor Y S, Williams A J, Checkelsky J G, Roushan P, Seo J, Xu Q, Zandbergen H W, Yazdani A, Ong N P and Cava R J 2010 *Phys. Rev. Lett.* **104** 057001
[15] Zhu X, Santos L, Sankar R, Chikara S, Howard C, Chou F C, Chamon C and El-Batanouny M 2011 *Phys. Rev. Lett.* **107** 186102
Luo C W *et al* 2013 *Nano Lett.* **13** 5797
Zhu X, Santos L, Howard C, Sankar R, Chou F C, Chamon C and El-Batanouny M 2012 *Phys. Rev. Lett.* **108** 185501
[16] Das Sarma S and Li Q 2013 *Phys. Rev.* B **88** 081404
[17] Pan Z-H, Fedorov A V, Gardner D, Lee Y S, Chu S and Valla T 2012 *Phys. Rev. Lett.* **108** 187001
Parente V, Tagliacozzo A, von Oppen F and Guinea F 2013 *Phys. Rev.* B **88** 075432
[18] Ali M N, Gibson Q D, Klimczuk T and Cava R J 2014 *Phys. Rev.* **B 89** 020505
[19] Hamlin J J, Jeffries J R, Butch N P, Syers P, Zocco D A, Weir S T, Vohra Y K, Paglione J and Maple M B 2012 *J. Phys.: Condens. Matter* **24** 035602
Kirshenbaum K, Syers P S, Hope A P, Butch N P, Jeffries J R, Weir S T, Hamlin J J, Maple M B, Vohra Y K and Paglione J 2013 *Phys. Rev. Lett.* **111** 087001
[20] Fu L and Berg E 2010 *Phys. Rev. Lett.* **105** 097001
[21] Lu C-K and Herbut I F 2010 *Phys. Rev.* B **82** 144505
Roy B, Juricic V and Herbut I F 2013 *Phys. Rev.* B **87** 041401
[22] Brydon P M R, Das Sarma S, Hui H-Y and Sau J D 2014 Odd-parity superconductivity from phonon-mediated pairing, arXiv:1402.7061v1
[23] White R M 1983 *Quantum Theory of Magnetism* (Heidelberg: Springer)
[24] Li D-P, Rosenstein B, Shapiro I and Shapiro B Ya 2014 *Phys. Rev.* B **90** 054517
[25] Sachdev S 2011 *Quantum Phase Transitions* 2nd edn (Cambridge: Cambridge University)
[26] Lee P A, Nagaosa N and Wen X-G 2006 *Rev. Mod. Phys.* **78** 17
[27] Li D, Rosenstein B, Shapiro I and Ya S B 2014 *Phys. Rev.* B **82** 144505
[28] Checkelsky J G, Hor Y S, Cava R J and Ong N P 2011 *Phys. Rev. Lett.* **106** 196801
Kim D, Cho S, Butch N P, Syers P, Kirshenbaum K, Adam S, Paglione J and Fuhrer M S 2012 *Nat. Phys.* **8** 459
[29] Abrikosov A A, Gor'kov L P and Dzyaloshinskii I E 1965 *Quantum Field Theoretical Methods in Statistical Physics* (New York: Pergamon)
Ketterson J B and Song S N 1999 *Superconductivity* (Cambridge: Cambridge University Press)
[30] Roy B, Sau J D and Das Sarma S 2014 *Phys. Rev.* B **89** 165119
[31] Zhang H, Liu C-X, Qi X-L, Dai X, Fang Z and Zhang S-C 2009 *Nat. Phys.* **5** 438
[32] Knigavko A and Rosenstein B 2003 *Phys. Rev. Lett.* **82** 1261
Knigavko A and Rosenstein B 1999 *Phys. Rev.* B **58** 935
Knigavko A, Rosenstein B and Chen Y F 1999 *Phys. Rev.* B **60** 5504
Li Q, Toner J and Belitz D 2009 *Phys. Rev.* B **79** 014517
Bel G, Rosenstein B, Ya S B and Shapiro I 2003 *Europhys. Lett.* **64** 503
Rosenstein B, Shapiro I, Shapiro B Ya and Bel G 2003 *Phys. Rev.* B **67** 224507